ME 326 Project 2: Boundary Layer Flow

Yurgen Hohmeyer[1]

[1]Department of Mechanical Engineering, Clarkson University

April 25th, 2021

Abstract

This project examines air flowing over a flat, horizontal stream-wise plate and the development of the boundary layer using ANSYS FLUENT commercial CFD code. Cases of laminar and turbulent flow were studied and compared to determine the behavior of boundary layer in different flow regimes. Furthermore, the FLUENT results were compared to theoretical results from the Blasius Similarity Solution and the one-seventh-power law. Result comparisons showed that commercial CFD code producing numerical solutions to the Navier-Stokes equations can show fluid behaviors not predicted by Blasius' solution and empirical equations, including a velocity "overshoot" near the edge of the boundary layer. Additionally, it was found that the Blasius solution provided many inaccuracies, especially near the beginning of the plate.

Contents

Nomenclature

C_D	Drag Coefficient	U_L	Laminar Inlet Velocity [$\mathrm{m\,s^{-1}}$]
C_f	Skin Friction Coefficient	U_T	Turbulent Inlet Velocity [$\mathrm{m\,s^{-1}}$]
I	Turbulence Intensity	δ	Boundary Layer Thickness [m]
Re	Reynolds Number	μ	Dynamic Viscosity [$\mathrm{kg\,m^{-1}\,s^{-1}}$]
U_o	Inlet Velocity [$\mathrm{m\,s^{-1}}$]	ρ	Fluid Density [$\mathrm{kg\,m^{-3}}$]

1 Introduction

Boundary layer flow refers to the layer of fluid found in close proximity to bounding surfaces in a flow. The presence of a boundary layer is due to the viscous forces in a flow, where, for example, the fluid "sticks" to a wall or other surface due to the no-slip condition. The concept of boundary layer flow was first discovered by Ludwig Prandtl in 1904 and has been developed extensively since [1]. However, no analytical solution to boundary layer equations are available. The first numerical solution was found in 1908 by P. R. Heinrich Blasius, which became known as the Blasius Similarity Solution [1].

In the present work, this so-called boundary layer that is created by fluid flowing over a flat plate is examined for different flow regimes using commercial CFD code, namely ANSYS FLUENT. The calculated results are also compared to Blasius' solution and empirical equations for turbulent boundary layer flow. Friction coefficients along the plate were also investigated and compared to determine the validity of analytical and empirical equations.

2 Experimental Setup

The analysis for this project was completed in two dimensions with a rectangular domain that was 30 centimeters tall by 1 meter long. The left edge of the domain was a velocity inlet where the flow entered normal to the edge, while the bottom edge was a no-slip flat plate (wall). The remaining top and right edges were pressure outlets. The problem domain is illustrated in Figure 1. A laminar case and turbulent case were studied, for which the inlet velocity was $0.02\,\mathrm{m\,s^{-1}}$ and $2\,\mathrm{m\,s^{-1}}$, respectively.

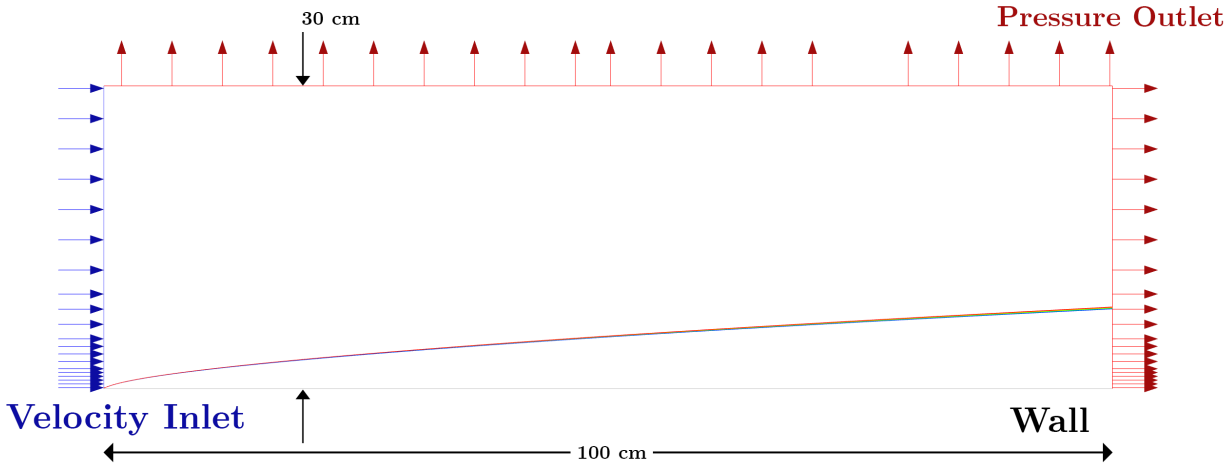

Figure 1: Problem domain with boundary conditions and dimensions.

The working fluid for the experiment was air modeled as an incompressible fluid with a density of $1.225\,\mathrm{kg\,m^{-3}}$ and a dynamic viscosity of $1.7894 \times 10^{-5}\,\mathrm{kg\,m^{-1}\,s^{-1}}$.

2.1 Numerical Solution Methodology

ANSYS FLUENT was used as the computational fluid dynamics (CFD) solver to obtain a numerical solution. After creating the 2D geometry, a mesh with quadrilateral faces was generated using an element size of $5 \times 10^{-3}\,\mathrm{m}$. To ensure solution accuracy and to obtain sufficient detail of the boundary layer created due to the flat plate, the mesh was refined near the plate in stages. The refined mesh is shown in Figure 2.

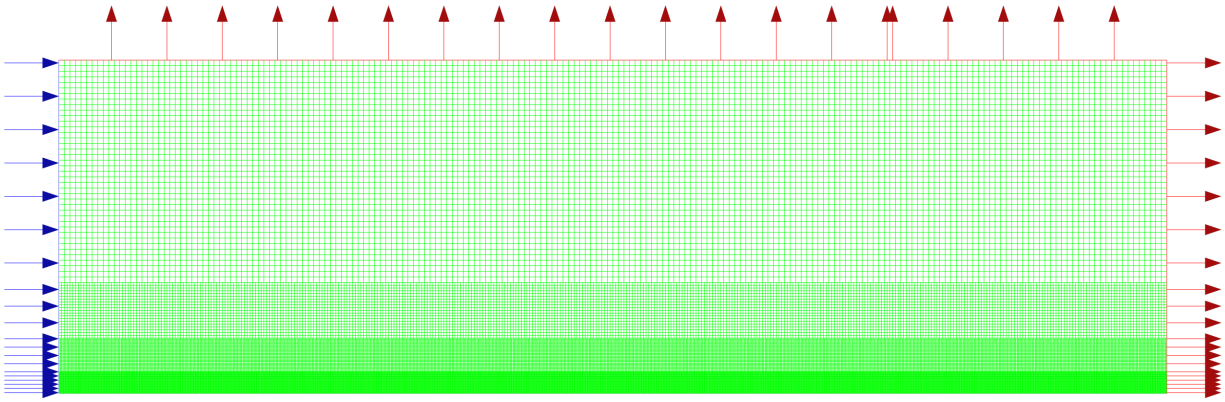

Figure 2: Mesh with staged refinements near the bottom edge.

The first refinement stage doubled the number of mesh elements up to 0.1 meters from the plate. The second stage doubled the number of elements again up to 0.05 meters from the wall, while the final stage doubled the elements a final time 0.025 meters from the wall. The resulting element sizes are reported in Table 1.

Table 1: Refined mesh element sizes.

Height Above Plate [m]	Element Size [m]
$0.000 \leq y < 0.025$	6.25×10^{-4}
$0.025 \leq y < 0.050$	1.25×10^{-3}
$0.050 \leq y < 0.100$	2.50×10^{-3}
$0.100 \leq y$	5.00×10^{-3}

2.1.1 Laminar

The laminar inlet velocity U_L was $0.02\,\mathrm{m\,s^{-1}}$. To be sure that the flow was in the laminar regime, the Reynolds number was calculated using

$$Re = \frac{\rho U L}{\mu} \tag{1}$$

where ρ is the fluid density, U is the flow velocity, L is the characteristic length scale of the geometry, and μ is the dynamic viscosity of the fluid. In the case of a flat plate, the characteristic length scale is the plate length. The Reynolds number was calculated to be 1369.2, confirming the flow to be in the laminar regime.[1]

[1] A flow is defined to be laminar if $Re < Re_{x,\mathrm{crit}}$ where $Re_{x,\mathrm{crit}} \approx 10^5$[1].

For the solution method in FLUENT, the pressure-velocity coupling scheme was set to SIMPLE with a standard spatial discretization method for pressure. The convergence monitors were also turned off, the solution took a standard initialization from the inlet properties, and the number of iterations was set to 3,000. The remaining FLUENT settings were left at their default values.

2.1.2 Turbulent

The solution methodology for the turbulent flow was duplicated from the laminar case. However, the inlet velocity U_T was $2.00\,\mathrm{m\,s^{-1}}$. The Reynolds number was again calculated using (1), which yielded a Reynolds number of 1.3692×10^5, categorizing the flow as transitional. Due to the transitional nature, the standard k-ϵ turbulent model was used. Additionally, the Turbulent Kinetic Energy and Turbulent Dissipation Rate were second order upwind. The specification method for the inlet velocity was also changed to "Intensity and Length Scale", where the turbulence intensity I of the flow was calculated using

$$I = 0.16 Re^{-1/8} \tag{2}$$

where Re is the Reynolds Number and the length scale was the plate length. Using the properties of the working fluid, the intensity was calculated to be

$$I = 0.16 \times \left(1.3692 \times 10^5\right)^{-1/8} = 0.03648 \tag{3}$$

or 3.648%. Finally, the solution was set to calculate for 5,000 iterations.

2.2 Theoretical Solution Methodology

The theoretical solution to determine the boundary layer over the posed flat plate was also calculated using the Blasius similarity solution for the laminar flow and two variations of the one-seventh-power law for the turbulent flow. The equations and MATLAB code for the boundary layer thickness, skin friction coefficient, and drag coefficient are detailed in Appendix B.

3 Results and Discussion

3.1 Solution Convergence

The refined mesh near the bottom of the domain caused both the laminar and turbulent solutions to have relatively slow convergence rates. For the laminar flow, the residual plot from FLUENT indicated that, after 3,000 iterations, the solutions for the x and y velocities only converged enough to lower the magnitude of the residuals to approximately 5×10^{-3}. The continuity residuals, however, were only about 5×10^{-7}. The turbulent flow solution converged further, yielding smaller residual values, as shown in Appendix A. The x and y velocity solutions converged enough to only have residual magnitudes on the order of 1×10^{-8} after 5,000 iterations. The residuals for k were on the order of 1×10^{-10}, while the residuals for continuity and ϵ were on the order of 1×10^{-12} and 1×10^{-14}, respectively.

3.2 Boundary Layer Features

3.2.1 Velocity

The velocity contours of the laminar and turbulent cases are reported in Figure 3. The boundary layer is visualized gradually grows across the length of the flat plate. The laminar flow contour of Figure 3a shows a thicker, more gradual boundary layer than that of the turbulent flow case in Figure 3b. This discrepancy is primarily due to the slower velocity of the laminar flow, where the no-slip condition and viscous forces on the flat plate have a more significant effect.

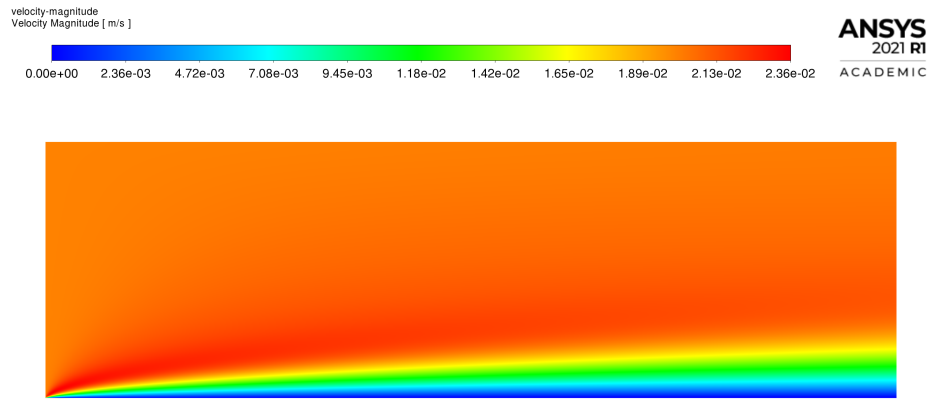

(a)

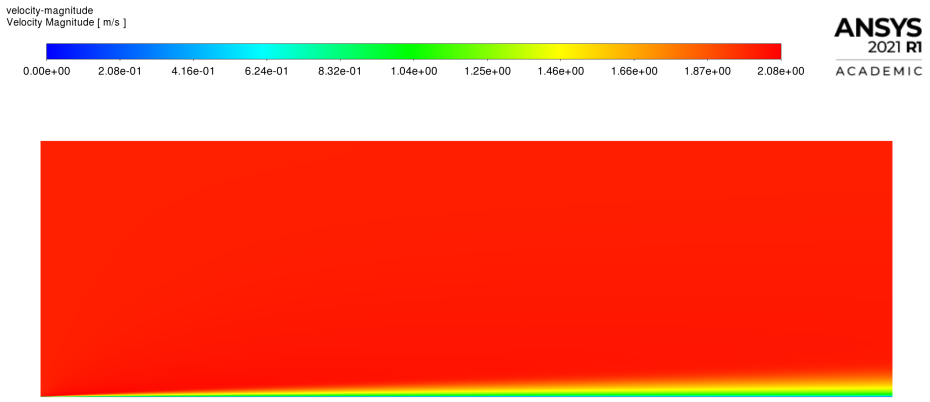

(b)

Figure 3: Velocity magnitude contours for laminar flow (a) and turbulent flow (b).

The difference in graduality between the laminar and turbulent boundary layers is shown further in Figure 4. In Figure 4a the height of the boundary layer is increasing across the plate, with a gradual transition at the top edge of the boundary layer back to the initial flow velocity. However, in Figure 4b the top-edge transition of the boundary layer is sharper, correlating to a more instantaneous transition and defined boundary layer.

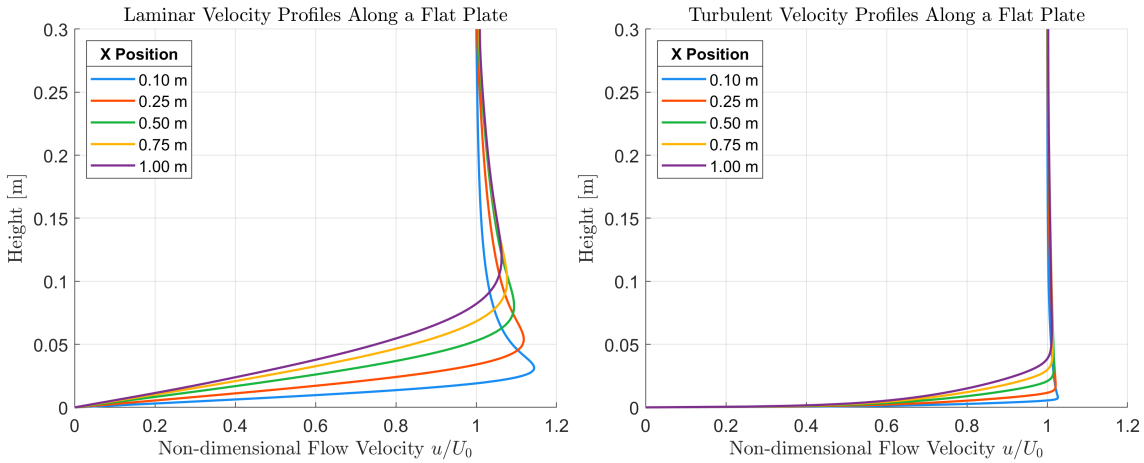

(a) (b)

Figure 4: Velocity profiles along the length of the flat plate for laminar (a) and turbulent flow (b).

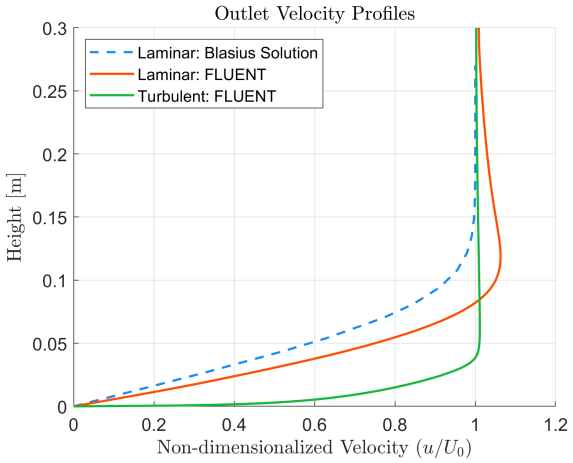

Figure 5: Outlet velocity for laminar, turbulent, and theoretical (Blasius) flows.

The boundary layer velocities at the end of the plate were also compared to the laminar Blasius Similarity Solution. The results of this comparison are reported in Figure 5, where the Blasius outlet velocity was plotted using values from the similarity solution which was solved using the Runge-Kutta numerical technique. The FLUENT solutions both shared an "overshoot" of the inlet velocity, where the maximum laminar velocity was $1.063U_L$ and the maximum turbulent velocity was $1.011U_T$. Compared to the Blasius approximation, this characteristic of the FLUENT solutions is unique. However, the discrepancy arises due to FLUENT numerically solving the full Navier-Stokes equations, whereas the Blasius solution is an approximation with neglected terms.

3.2.2 Thickness

The boundary layer thickness is defined as $0.99U_o$, where U_o is the inlet velocity. To obtain boundary layer height contours in FLUENT, the velocity magnitude was plotted between $0.985U_o$ and $0.995U_o$. The resulting contours are shown in Figure 6. Additionally, the laminar Blasius similarity solution boundary layer thickness is plotted alongside the approximate turbulent boundary layer solutions of (5) and (6).

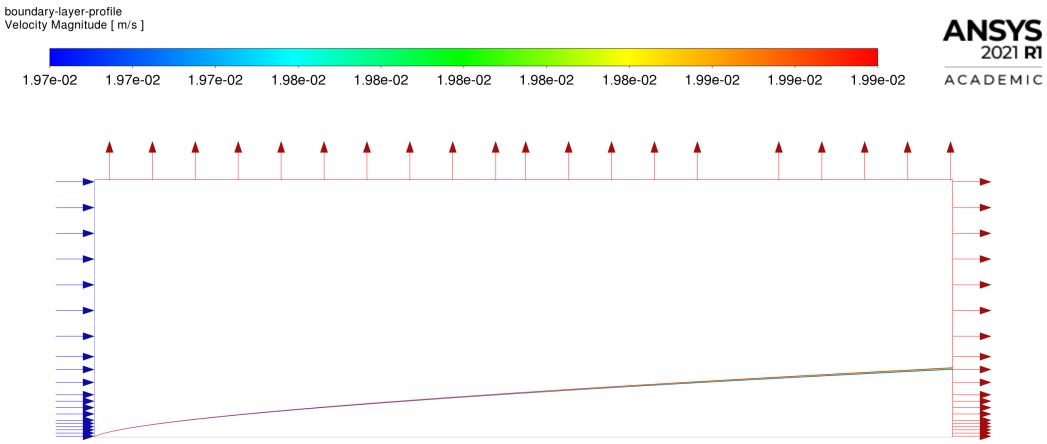

(a)

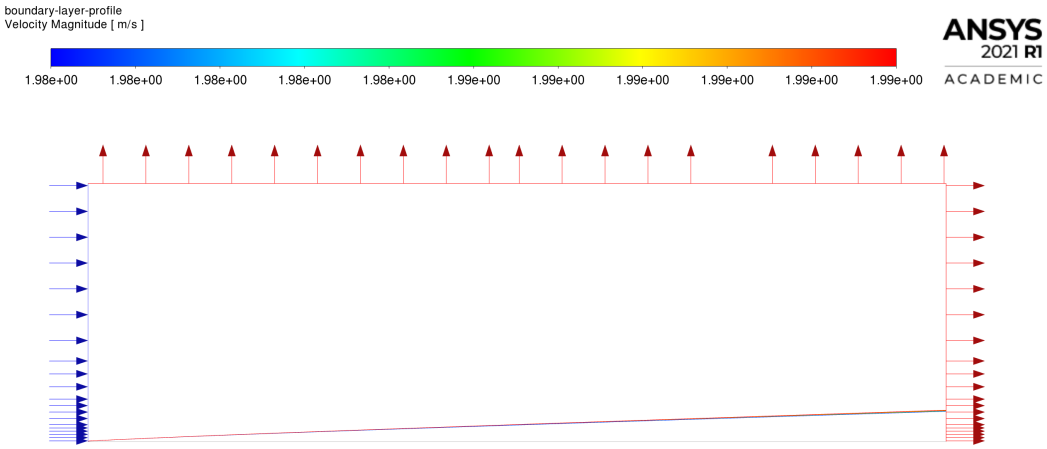

(b)

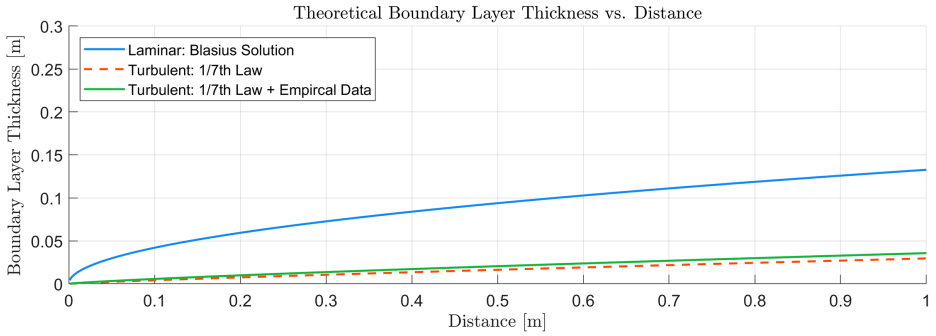

(c)

Figure 6: Boundary layer contours for laminar (a), turbulent (b), and theoretical laminar and turbulent flow (c).

Comparing the graphical results shows that, for a flat plate, the Blasius solution and the one-seventh-power laws are decent approximations of the flow. However, to determine the true boundary layer thickness, the previous results were interpolated to find the approximate height above the plate at which δ became $0.99U_o$ for each case. The findings of which are reported and compared in Table 2. The percent-difference between the Blasius approximation and CFD calculated values verified the observation visible in examining Figure 6

— the Blasius solution is not exact, but is within 56% of the exact value. The one-seventh-power law for turbulent flow is closer to the CFD value, coming within 7% of the calculated value. Equation 6 was developed using the one-seventh law in conjunction with empirical data. However, the empirical data used was from turbulent flow through smooth pipes [1], not over a flat plate, which is likely where the higher inaccuracy compared to the standard one-seventh law is developed from.

Table 2: Boundary layer thickness results.

Position (x)	**Laminar B.L. Thickness [cm]**			**Turbulent B.L. Thickness [cm]**				
	CFD	Blasius	Difference	CFD	1/7th Law[2]	Difference	1/7th Law+[3]	Difference
0.01	1.871	4.196	55.4%	0.5265	0.5656	6.91%	0.4104	28.3%
0.25	3.332	6.635	49.8%	1.095	1.177	6.97%	0.9001	21.7%
0.50	5.167	9.383	44.9%	1.943	2.050	5.22%	1.630	19.2%
0.75	6.665	11.49	42.0%	2.748	2.835	3.07%	2.308	19.1%
1.00	7.990	13.27	39.8%	3.521	3.569	1.34%	2.954	19.2%

3.3 Friction and Drag

The skin friction coefficient (C_f) for the laminar and turbulent FLUENT results, as well as theoretical values, is reported in Figure 7. The Blasius solution underestimated the laminar CFD solution by an average of 3.091×10^{-2}, while the one-seventh law and the semi-empirical one-seventh law underestimated the turbulent CFD solution by an average of 5.774×10^{-3} and 4.673×10^{-3}, respectively. The converged C_f and drag coefficient (C_D) values present at the end of the flat plate are reported in Table 3. The percentage-difference between the CFD and theoretical friction coefficients is greater than the percent-difference of the boundary layer thickness. As the friction coefficient equations are also derived from the Blasius solution and the one-seventh law, this is to be expected.

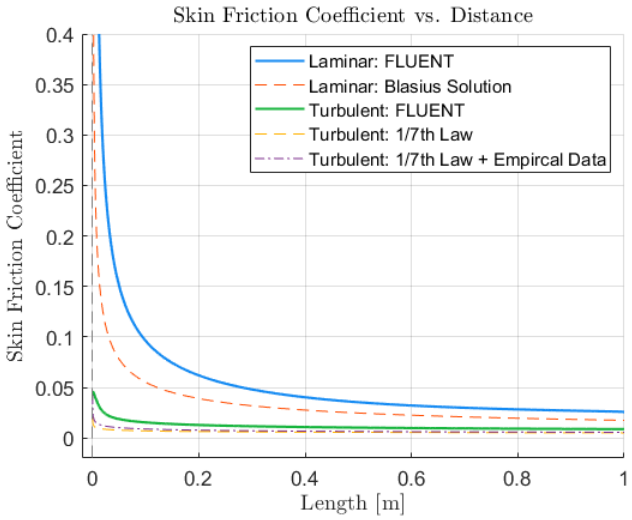

Figure 7: Skin friction coefficient for laminar and turbulent flows.

Table 3: Converged friction coefficients.

Coefficient	**Laminar**			**Turbulent**				
	CFD	Blasius	Difference	CFD	1/7th Law	Difference	1/7th Law+	Difference
Friction (C_f)	0.02564	0.01740	47.4%	0.008648	0.004984	73.5%	0.005541	56.1%
Drag (C_D)	0.06358	0.03589	77.2%	0.011570	0.006949	66.5%	0.005722	102%

[2]Standard one-seventh-power law.
[3]One-seventh-power law equation developed from the standard equation and empirical data.

4 Conclusions

Commercial CFD code was used to analyze the
boundary layer flow over a flat plate and compared to approximate solutions. Though Prandtl's boundary layer approximation was a major breakthrough in the early 1900s and Blasius' similarity solution allowed for an early approximation of boundary layer flow, the progression of technology has allowed for more accurate solutions. Results showed that CFD code such as ANSYS FLUENT numerically solving the Navier-Stokes equations provide more accurate solutions to the boundary layer phenomenon. This was especially evident in the velocity profiles, where the numerical Navier-Stokes solutions presented a velocity "overshoot" where the boundary layer fluid velocity exceeded the inlet velocity, which was not present in the theoretical solutions.

Prandtl's approximations assumed several terms in the Navier-Stokes equations that are important at the beginning of the boundary layer to be negligible, which causes inaccuracies in the Blasius solution near the beginning of the plate. However, near the end of the plate Blasius' solution came within 40% of the CFD value for the boundary layer thickness. The turbulent boundary layer equations were among the most accurate theoretical equations for boundary layer thickness, which were within 2% of the CFD value at the end of the plate. The theoretical friction coefficients were found to be fairly inaccurate, ranging in percent difference of 47.4% to 102%. However, the turbulent flow Reynolds Number is just inside the transitional flow region, which could cause inaccuracies using equations for fully turbulent flows.

References

[1] John M. Cimbala Yunus A.Çengel. *Fluid Mechanics: Fundamentals and Applications*. Fluid Mechanics. McGraw Hill Education, 2017. ISBN: 978-1-259-69653-4.

A Appendix: ANSYS FLUENT Residuals

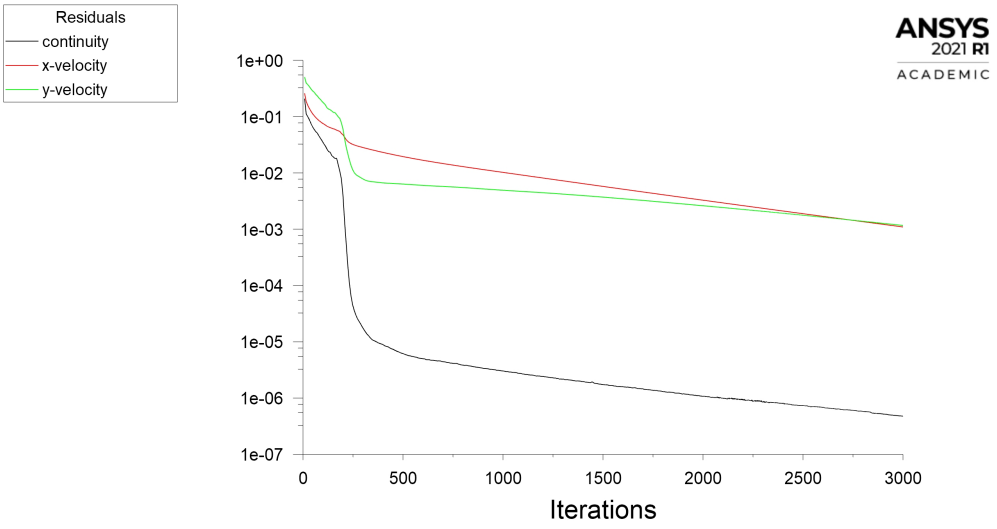

Figure 8: Numerical calculation residuals for laminar flow over a flat plate from ANSYS FLUENT.

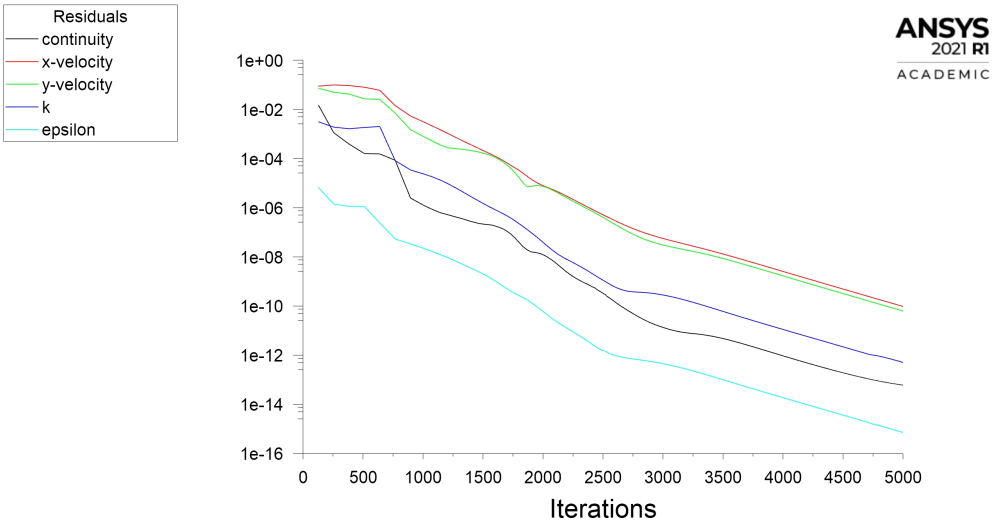

Figure 9: Numerical calculation residuals for turbulent flow over a flat plate from ANSYS FLUENT.

B Appendix: Theoretical Boundary Layer Solution

The Blasius solution defines the laminar boundary layer thickness, δ_L, as

$$\delta_L = \frac{4.91x}{\sqrt{Re_x}} \tag{4}$$

For turbulent flow, the one-seventh power law defines the approximate boundary layer thickness as

$$\delta_{T1} \approx \frac{0.16x}{(Re_x)^{1/7}} \tag{5}$$

and the one-seventh power law combined with empirical data approximates the thickness as

$$\delta_{T2} \approx \frac{0.38x}{(Re_x)^{1/5}} \tag{6}$$

These equations were then solved over the problem domain. Definitions for the laminar friction coefficient

$$C_{f,L} = \frac{0.644}{\sqrt{Re_L}} \tag{7}$$

and the turbulent friction coefficient using the one-seventh-power law

$$C_{f,T1} \approx \frac{0.027}{Re_T^{1/7}} \tag{8}$$

and the empirical one-seventh-power law

$$C_{f,T2} \approx \frac{0.059}{Re_T^{1/5}} \tag{9}$$

were also used for the theoretical solution. One additional parameter, the coefficient of drag, was also of interest and defined as

$$C_{D,L} = \frac{1.328}{\sqrt{Re_L}} \tag{10}$$

for laminar flow and

$$C_{D,T1} \approx \frac{0.031}{Re_T^{1/7}} \tag{11}$$

and

$$C_{D,T2} \approx \frac{0.074}{Re_T^{1/5}} \tag{12}$$

for turbulent flow.

The above equations were then defined as functions in a MATLAB script, which allowed them to be plotted over the problem domain and compared to the CFD results. Further, using Blasius' similarity solution,

$$\eta = y\sqrt{\frac{U}{\nu x}} \tag{13}$$

where η is the similarity variable, y is the height above the plate, U is the fluid velocity, ν is the kinematic viscosity, and x is the distance along the plate, and solving for y, it was found that

$$y = \frac{\eta}{\sqrt{U_L/(\nu L)}} \tag{14}$$

Finally, the numerically solved similarity values for

$$f' = \frac{u}{U} \tag{15}$$

were used to plot the non-dimensional velocity of the Blasius solution. A high-level overview of the MATLAB code and similarity solution values are shown in Listing 1.

```
%% Theoretical Functions
% Reynolds number
ReL = @(x) rho*U_L.*x/mu;
ReT = @(x) rho*U_T.*x/mu;

% Boundary layer thickness [m]
BLT_L = @(x) 4.91.*x./sqrt(ReL(x));
BLT_T1 = @(x) 0.38.*x./ReT(x).^(1/5);
BLT_T2 = @(x) 0.16.*x./ReT(x).^(1/7);

% Skin friction coefficient
C_fL = @(x) 0.644./sqrt(ReL(x));
C_fT1 = @(x) 0.027./ReT(x).^(1/7);
C_fT2 = @(x) 0.059./ReT(x).^(1/5);

% Drag coefficient
C_DL = @(x) 1.328./sqrt(ReL(x));
C_DT1 = @(x) 0.074./ReT(x).^(1/5);
C_DT2 = @(x) 0.031./ReT(x).^(1/7);

%% Blasius Solution Velocity Profile
% f Prime Values
Blasius_fp = [0 0.16589 0.32978 0.51676 0.62977 0.77245 0.84604 0.91304...
              0.95552 0.97951 0.99154 0.99688 0.99897 0.99970 0.99992...
              1.00000 1.00000 1.00000];
% Similarity Variable Values
Blasius_eta = [0 0.5 1 1.6 2.0 2.6 3.0 3.5 4.0 4.5 5.0 5.5 6.0 6.5 7.0 8.0 9.0 10.0];
% Height Values
Blasius_y = Blasius_eta/sqrt(U_L/(nu*L));
```

Listing 1: Sample MATLAB Code